

Spatial Array Processing in a 3D Multiuser Network

Johanna Ketonen, Xiaojia Lu and Markku Juntti
Centre for Wireless Communications
University of Oulu, Finland
{johanna.ketonen, markku.juntti}@ee.oulu.fi

Abstract

The performances of spatial array processing algorithms along with three-dimensional (3D) antenna arrays are studied in this paper. Optimal linear beamforming is compared to codebook based processing. The elevation domain is further utilized when applying separate weighting vectors for the azimuth and elevation dimensions. The theoretical capacities of the beamforming systems with different antenna arrays are compared. Simulations are performed with the latest 3D channel models in a multiuser network. The best performance is obtained with the horizontal uniform linear arrays (ULA) when optimal beamforming is used. However, the performances of ULA and uniform planar array (UPA) are similar when codebook based beamforming is employed.

I. INTRODUCTION

The demand for higher spectral efficiency in wireless communication systems has been growing due to the increased data rate and quality of service requirements. One solution has been to place antennas in a three dimensional (3D) space in the base station (BS). This enables the utilization of the elevation domain in beamforming. An individual beam pattern can be assigned to each user in both elevation and azimuth domains. Field trials in [1] showed major improvements in system performance when separating the simultaneous transmissions to different users in the elevation domain.

The spatial correlation and capacity for rectangular arrays were discussed in [2]–[4]. Both the azimuth-of-arrival (AOA) and elevation-of-arrival (EOA) were shown to affect the spatial correlation of uniform rectangular arrays in [2] with the AOA having the highest impact. Two-dimensional channel models have been used extensively in multiple antenna research. Recently, those models have been extended to three-dimensional ones. The WINNER II project proposed a 3D channel model in [5] which was not based on extensive measurements. The Third Generation Partnership Project (3GPP) presented a three-dimensional model in [6] more recently.

The uniform planar arrays (UPA) and the uniform linear arrays (ULA) were compared in [7] via system level simulations. The UPA was found to perform better in interference limited scenarios but the difference between the two arrays grew smaller as the number of cooperating BSs increased. However, the geometries of the ULA and UPA were the same and the WINNER II model was used in [7]. The performance of different types of antenna arrays utilizing the latest channel models while taking into account different beamforming

techniques and their complexities have not been discussed in the literature.

In this paper, the 3D channel models are utilized when comparing the performances of different beamforming techniques with different antenna arrays, namely the UPA and ULA. 3D MIMO is studied both from point-to-point and system level view. Comparisons between the ULA and UPA are first made with their spatial correlation functions. The performance is then simulated with the most recent 3D channel model and multicell network simulations. The theoretical complexity of beamforming weight calculation is then reported.

The rest of the paper is organized as follows. The system and channel models are presented in II. The spatial correlation and beamforming capacities are reported in III and the array processing algorithms are introduced in IV. Performance examples are given in V and complexity results are discussed in VI. Conclusions are finally drawn in VII.

II. SYSTEM AND CHANNEL MODEL

A. Multicell System

The considered cellular system consists of K MSs and B BSs in flat fading channels. All MSs have one transmit antenna while BS i has N_i receive antennas. The received signal $\mathbf{r}_i \in \mathbb{C}^{N_i \times 1}$ at the i th BS is written as

$$\mathbf{r}_i = \sum_{k=1}^K \sqrt{p_k} \mathbf{h}_{k,i} s_k + \mathbf{n}_i, \quad (1)$$

where p_k is the transmit power of MS k , s_k is the transmitted symbol of MS k with average power normalized to 1, $\mathbf{h}_{ij} \in \mathbb{C}^{N_i \times 1}$ is the complex channel response from the k th MS to the i th BS and $\mathbf{n}_i \in \mathbb{C}^{N_i \times 1}$ is the additive white Gaussian noise (AWGN) vector at BS i with variance σ_i^2 for each receive antenna.

B. 3D Spatial Channel

The 3D channel model is based on the WINNER II channel model which is a geometry based stochastic model [8]. A general form of MIMO channel matrix is given by

$$\mathbf{H}(t, \tau) = \sum_{n=1}^N \mathbf{H}_n(t; \tau), \quad (2)$$

where n is the path index, t is the time index, N is the total number of paths, and τ is the delay time. $\mathbf{H}_n(t, \tau)$ is the channel matrix for cluster n which is expressed as [8]

$$\mathbf{H}_n(t; \tau) = \int \mathbf{F}_{\text{Rx}}(\phi) \mathbf{H}(t; \tau, \phi, \varphi) \mathbf{F}_{\text{Tx}}^T(\varphi) d\phi d\varphi, \quad (3)$$

where $F_{\text{Rx}}(\phi)$ and $F_{\text{Tx}}(\varphi)$ are the beam gain matrix for receiver (Rx) and transmit antenna (Tx) on directions ϕ and φ , respectively. $H(t; \tau, \phi, \varphi)$ is the dual-polarized channel response matrix. The channel coefficient from Tx s to Rx element u for cluster n is given as [8]

$$h_{u,s,n}(t; \tau) = \sum_{m=1}^M \begin{bmatrix} F_{\text{Rx},u,V}(\varphi_{n,m}) \\ F_{\text{Rx},u,H}(\varphi_{n,m}) \end{bmatrix} \begin{bmatrix} \alpha_{n,m}^{VV} & \alpha_{n,m}^{VH} \\ \alpha_{n,m}^{HV} & \alpha_{n,m}^{HH} \end{bmatrix} \begin{bmatrix} F_{\text{Tx},u,V}(\phi_{n,m}) \\ F_{\text{Tx},u,H}(\phi_{n,m}) \end{bmatrix} \times \exp(j2\pi\lambda_0^{-1}(\bar{\varphi}_{n,m} \cdot \bar{r}_{\text{Rx},u})) \exp(j2\pi\lambda_0^{-1}(\bar{\phi}_{n,m} \cdot \bar{r}_{\text{Tx},s})) \times \exp(j2\pi v_{n,m}t) \delta(\tau - \tau_{n,m}), \quad (4)$$

where $\alpha_{n,m}^{VV}$ and $\alpha_{n,m}^{VH}$ are the complex gains of vertical-to-vertical and horizontal-to-vertical polarizations of ray n , m respectively and $F_{\text{Rx},u,V}$ and $F_{\text{Rx},u,H}$ are the field patterns for vertical and horizontal polarizations of antenna element u respectively. Parameter λ_0 is the wave length of the carrier frequency, $\bar{\phi}_{n,m}$ is the angle of departure (AoD) unit vector, $\bar{\varphi}_{n,m}$ is the angle of arrival (AoA) unit vector, $\bar{r}_{\text{Tx},s}$ and $\bar{r}_{\text{Rx},u}$ are the location vectors of elements s and u respectively, and $v_{n,m}$ is the Doppler frequency of ray n , m . If polarization is not considered, the central matrix in the second line of (4) is replaced by a scalar $\alpha_{n,m}$ and only vertically polarized field pattern is considered. More details on the channel model can be found in [8].

The radiation antenna pattern in the azimuth angle direction [9] is given as

$$A_A(\theta) = -\min \left[12 \left(\frac{\theta}{\theta_{3\text{dB}}} \right)^2, A_m \right], \quad -180^\circ \leq \theta \leq 180^\circ, \quad (5)$$

where $\theta_{3\text{dB}}$ is the 3dB beamwidth which is 65° for 3-sector cell and $A_m = 30\text{dB}$ is the maximum attenuation. In the elevation angle direction, the radiation antenna pattern is expressed as

$$A_E(\gamma) = -\min \left[12 \left(\frac{(\gamma - 90 \text{ deg} - \gamma_{\text{tilt}})}{\gamma_{3\text{dB}}} \right)^2, A_m \right], \quad (6)$$

where $\gamma_{3\text{dB}} = 65^\circ$ is the 3 dB vertical beamwidth and $0^\circ \leq \gamma \leq 180^\circ$.

C. Antenna Array

An illustration of the antenna coordination system and an incident wave is shown in Fig. 1.

The spatial displacement of the receive and transmit antenna elements and phase shifts among them is included in terms of $\exp(j2\pi\lambda_0^{-1}(\bar{\varphi}_{n,m} \cdot \bar{r}_{\text{Rx},u}))$ and $\exp(j2\pi\lambda_0^{-1}(\bar{\phi}_{n,m} \cdot \bar{r}_{\text{Tx},s}))$ in (4), where $\bar{r}_{\text{Rx},u} = [x_u, y_u, z_u]^T$ is the location of the u th antenna element. The unit position vector is

$$\bar{\varphi} = [\cos \theta \cos \gamma, \sin \theta \cos \gamma, \sin \gamma]^T, \quad (7)$$

where θ is the arrival azimuth angle and γ is the arrival elevation angle. The phase delay of element u can be calculated as

$$v_u(\gamma, \theta) = \bar{\varphi} \cdot \bar{r}_{\text{Rx},u} = (x_u \cos \theta \cos \gamma + y_u \sin \theta \cos \gamma + z_u \sin \gamma). \quad (8)$$

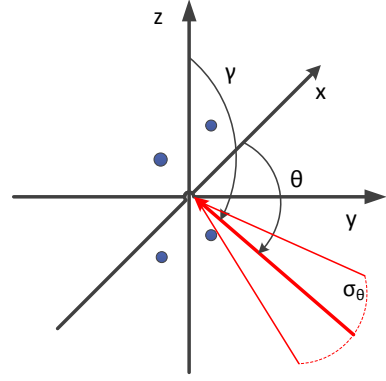


Fig. 1. An illustration of antenna coordination system.

III. SPATIAL CORRELATION OF ULA AND UPA

In this section, the impact of the elevation domain in point-to-point, single user MIMO is studied. Closed-form expressions for the spatial correlation functions for 3D antenna arrays were derived in [4]. The elevation and azimuth angles were assumed uniformly distributed. The spatial correlation between the u th and v th array element is given by [2]

$$R_s(u, v) = E\{v_u(\gamma, \theta)v_v^*(\gamma, \theta)\} = \int_{\gamma} \int_{\theta} v_u(\gamma, \theta)v_v^*(\gamma, \theta)p(\gamma, \theta) \sin \gamma d\gamma d\theta, \quad (9)$$

where $p(\gamma, \theta)$ is the angular distribution function of the incoming plane wave. The closed-form approximation of the spatial correlation function between the u th and v th antenna elements with uniformly distributed γ and θ can be found in [4].

The average correlation between the antenna elements in UPA and ULA as a function of the elevation or azimuth spreads are shown in Fig. 2. The central elevation and azimuth angles are 90° and the angle spreads are uniformly distributed. The antenna spacing is 0.5λ . The changes in elevation spread do not have an impact on the ULA. As the elevation spread increases, the correlation in the UPA decreases. The increase in azimuth spread decreases the correlation in both the ULA and UPA.

The random capacity of a beamforming system can be written as [10]

$$C = \log_2 \left(1 + N \frac{\text{SNR}}{2} \lambda_s \right), \quad (10)$$

where λ_s is the maximum singular value of R_s .

The capacity of a 16 transmit antenna beamforming system using (9) and (10) is illustrated in Fig. 3. The antenna spacing is 0.5λ . The capacity of the horizontal ULA does not change when the elevation spread increases but decreases when the azimuth spread increases. The result is opposite in the vertical ULA. The same result can be seen for the UPA as the capacity decreases with the increase in elevation spread but no change is observed when the azimuth spread increases.

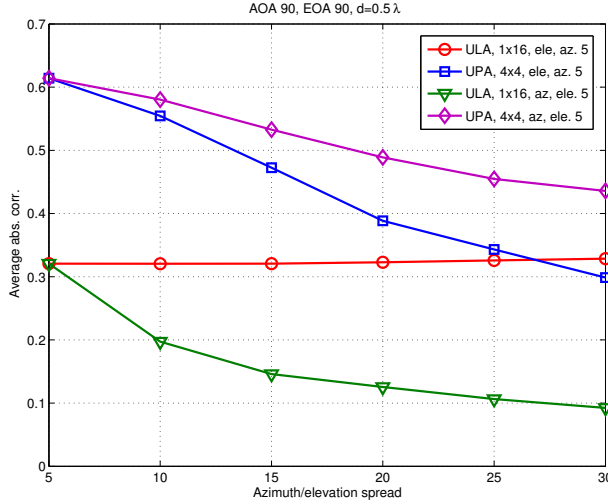


Fig. 2. Average correlation between the antenna elements.

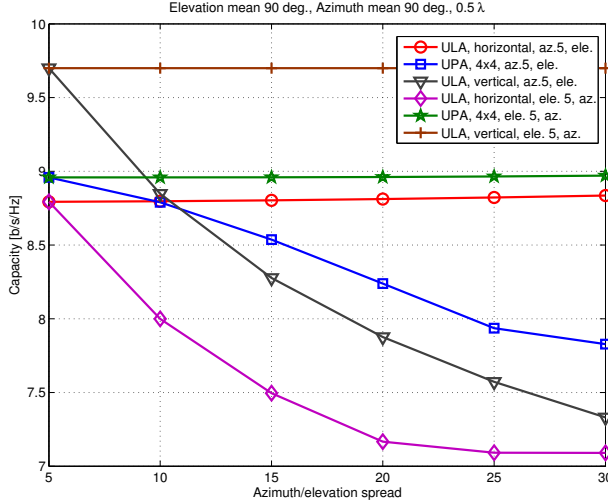


Fig. 3. Capacity of a beamforming system.

IV. ARRAY PROCESSING ALGORITHMS

The 3D MIMO from a system level point of view is studied via different beamforming techniques and multicell network simulations. Different beamforming weight calculation techniques were used when comparing the performances of the 3D antenna arrays. The optimal beamforming is compared to the codebook based beamforming. Separate beamforming weights for azimuth and elevation domains are also applied. The uplink power control and beamforming is performed similarly in all techniques.

Given the receiver beamformers $\mathbf{w}_{k,i}$ and the cooperation BS set π_k , the power control, BS cooperation reception and

beamforming problem can be formulated as

$$\begin{aligned} & \underset{\pi_k, p_k}{\text{minimize}} && \sum_{k=1}^K p_k \\ & \text{subject to} && \frac{\left| \sum_{i \in \pi_k} \mathbf{w}_{k,i}^H \mathbf{h}_{k,i} \right|^2 p_k}{\sum_{k' \neq k} \left| \sum_{i \in \pi_k} \mathbf{w}_{k,i}^H \mathbf{h}_{k',i} \right|^2 p_{k'} + \sum_{i \in \pi_k} \|\mathbf{w}_{k,i}\|^2 \sigma_i^2} \geq \varphi_k, \\ & && p_k \leq P_k \end{aligned} \quad (11)$$

where $|\cdot|$ denotes the absolute value, $\|\cdot\|$ the standard Euclidean vector norm, φ_k is MS k 's SINR requirement and P_k is the maximum transmit power of MS k . The optimal beamforming vector is given by

$$\begin{aligned} & \{\mathbf{w}_{k,1}, \mathbf{w}_{k,2}, \dots, \mathbf{w}_{k,|\pi_k|}\} = \\ & \arg \max_{\mathbf{w}_{k,i}} \frac{\left| \sum_{i \in \pi_k} \tilde{\mathbf{w}}_{k,i}^H \mathbf{h}_{k,i} \right|^2 \tilde{p}_k}{\sum_{k' \neq k} \left| \sum_{i \in \pi_k} \tilde{\mathbf{w}}_{k,i}^H \mathbf{h}_{k',i} \right|^2 \tilde{p}_{k'} + \sum_{i \in \pi_k} \|\tilde{\mathbf{w}}_{k,i}\|^2 \sigma_i^2} \end{aligned} \quad (12)$$

The minimum total transmit power solution, the optimal receiving BSs set and the optimal beamforming vector can be found after iterative search, as long as the power vectors of the MSs are feasible. A more detailed description of the algorithm can be found in [11]. When assuming only one base station, i.e., no cooperation, the set π_k includes only the serving base station and the index i can be omitted.

For the baseline case, the optimal beamforming vectors are calculated as the MMSE filter and a general form is given as

$$\mathbf{w} = (p\mathbf{h}\mathbf{h}^H + \sigma_i^2\mathbf{I})^{-1}\mathbf{h}. \quad (13)$$

For a simplified case, the beamforming vectors are taken from a codebook and the MS calculates the best beamforming vector. It is assumed that the MS knows the channel and it selects the beamforming vector based on channel capacity. The codebook for the 16 transmit and one receive antenna case was extended from the codebook for 8 transmit antennas in [12]. The codebook is given in Table I.

Different weighting vectors can be applied to the azimuth and elevation dimensions. For the case of 16 transmit antennas in the base station, a 4×1 weighting vector is used for both dimensions. The azimuthal weighting vectors are then chosen from the LTE codebook [13]. Two methods for finding the elevation weighting vectors were used. In the first method, a set of fixed elevation weighting vectors were applied. The coefficients for the weighting vectors $\mathbf{w}_V = [w_{V,1}, w_{V,2}, \dots, w_{V,n_V}]$ were given as [14]

$$w_{V,c} = \frac{1}{\sqrt{n_V}} [j2\pi(c-1)\frac{d_V}{\lambda} \cos \tilde{\gamma}], c = 1, \dots, n_V, \quad (14)$$

where n_V is the number of antennas placed in the elevation dimension, d_V is the antenna spacing in elevation, λ is the wave length of carrier frequency and $\tilde{\gamma}$ is the angle of the steering beam.

In the second method, the elevation weighting vector is calculated as the eigenvector corresponding to the largest

TABLE I
CODEBOOK FOR 16 TRANSMIT ANTENNAS

w_0	[1 1 1 1 1 1 1 1 1 1 1 1 1 1 1 1]
w_1	[1 q4 q3 q5 -j q6 q2 q7 -1 q8 q1 q9 j q10 q0 q11]
w_2	[1 -j -1 j 1 -j -1 j 1 -j -1 j 1 -j -1 j]
w_3	[1 q5 q2 q8 j q11 q4 -j q7 q1 q10 q3 q6 -1 q9 q0]
w_4	[1 -1 1 -1 1 -1 1 -1 1 -1 1 -1 1 -1 1]
w_5	[1 q0 q9 -1 q6 q3 q10 q1 q7 -j q4 q11 j q8 q2 q5]
w_6	[1 j -1 -j 1 j -1 -j 1 j -1 -j 1 j -1 -j]
w_7	[1 q11 q0 q10 j q9 q1 q8 -1 q7 q2 q6 -j q5 q3 q4]
w_8	[q0 q11 q11 1 1 q4 q4 q3 q3 q5 q5 -j j q6 q6 q2]
w_9	[q0 1 q4 q5 -j q2 q7 q8 q1 j q10 q11 1 q3 q5 q6]
w_{10}	[q0 -j -1 q0 q3 -1 j q3 q0 -j -1 q0 q3 -1 j q3]
w_{11}	[q0 q2 j -j q1 q3 -1 1 q10 q6 q8 q4 q11 q7 q9 q5]
w_{12}	[q0 -1 1 q1 q3 j -j q9 q5 q11 q7 q8 q4 q0 q10 q6]
w_{13}	[q0 j q8 q7 -j q3 q11 q10 q1 -1 q6 q5 1 q0 q9 q8]
w_{14}	[q0 q10 q9 q1 -1 q7 q6 -j q3 q4 q11 q0 j q9 q8 -1]
w_{15}	[q0 q0 q10 q10 j j q9 q9 q1 q1 q8 q8 -1 -1 q7 q7]
$q0=(1+j)/\sqrt{2}, q1=(-1+j)/\sqrt{2}, q2=(-1-j)/\sqrt{2}, q3=(1-j)/\sqrt{2}$	
$q4=(1-0.5j)/\sqrt{2}, q5=(0.5-j)/\sqrt{2}, q6=(-0.5-j)/\sqrt{2}, q7=(-1-0.5j)/\sqrt{2}$	
$q8=(-1+0.5j)/\sqrt{2}, q9=(-0.5+j)/\sqrt{2}, q10=(0.5+j)/\sqrt{2}, q11=(1+0.5j)/\sqrt{2}$	

eigenvalue of $\mathbf{h}_a \mathbf{h}_a^H$, where $\mathbf{h}_a = \mathbf{h}_H \mathbf{I}_{n_H}$, \mathbf{h}_H is the channel vector corresponding to the azimuthal antennas, n_H is the number of antenna element placed on the azimuth dimension and \mathbf{I}_{n_H} is a vector of ones [15]. The power control and beamforming procedure with different beamforming methods is summarized in Table II.

TABLE II
POWER CONTROL AND BEAMFORMING

Initialization:
Set iteration index $t = 0$ and $p_k^{[0]} = 0$.
1. Set $t = t + 1$ for each k
2. Obtain w_k with (a), (b), (c) or (d)
(a) Calculate w_k as (13)
(b) Assume user selected w from codebook in Table I
(c) Assume user selected w_H from LTE codebook. Calculate w_V as in (14).
(d) Assume user selected w_H from LTE codebook. Calculate w_V as eigenvector corresponding to $\max\{eig(\mathbf{h}_a \mathbf{h}_a^H)\}$
3. Calculate p_k under SINR constraint φ_k as
$p_k = \frac{\sum_{k' \neq k} w_k^H \mathbf{h}_{k'} ^2 \tilde{p}_k^{[t-1]} + \ w_k\ ^2 \sigma^2}{ w_k^H \mathbf{h}_k ^2} \varphi_k$
4. Update $\tilde{p}_k^{[t]} = p_k^{[t]}$
5. If any $\tilde{p}_k^{[t]} > P_k$, SINR constraint is infeasible. Stop iterations.
6. If $ \sum_{i=1}^K \tilde{p}_k^{[t]} - \sum_{i=1}^K \tilde{p}_k^{[t-1]} < \epsilon$, stop and give the result. Else, go to step 1.

V. PERFORMANCE EXAMPLES

The performance of the ULA and UPA arrays with different beamforming methods is compared via computer simulations. A cellular system with 19 base stations is considered. Each BS has 3 sectors, i.e. there are of 57 sectors in total. Wrap around is used to eliminate the edge effect [16]. The simulation parameters are summarized in Table III. The cumulative distribution functions (CDF) of the transmit powers are shown in the following figures.

TABLE III
SIMULATION PARAMETERS

Layout	19 cells, 3 sectors/cell
Channel model	Urban Macro/Micro cell
Cell radius	1000 m
Maximum MS transmit power	24 dBm
Maximum antenna gain	17 dBi
Thermal noise density	-174 dBm/Hz
Shadow fading	Log-Normal, 8 dB standard deviation
Shadowing correlation	Independent
Down tilt angle	4/8 degree
SINR constraint per MS	0 dB
Number of users	10 in 19 cells
BS/MS antenna elements	16/1

The performances with ULA and UPA arrays and optimal beamforming with the Urban Micro and Macro cell channels are presented in Fig. 4. In both cases, the horizontal ULA performs better than the UPA or the vertical ULA. This can also be observed from Fig. 3. The performance in the Urban Macro cell is also better than in the Micro cell due to the higher BS and smaller elevation angles.

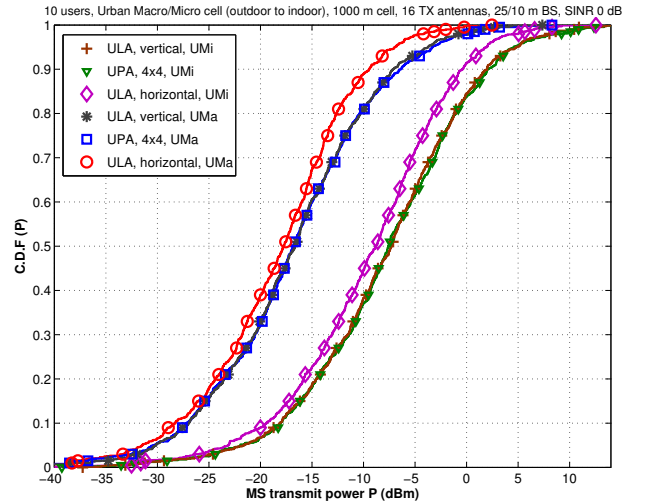


Fig. 4. Transmit power of ULA and UPA with 10 users, optimal beamforming and Urban Macro/Micro cell scenario.

In order to compare the results in Fig. 4 to the theoretical capacity in Fig. 3, the distributions of elevation angles of arrival for Urban Macro and Micro cell scenarios are shown in Fig. 5. It can be seen in Fig. 3, that the horizontal ULA outperforms the UPA and the vertical ULA when the elevation spread increases. The elevation angles have a fairly large spread in Fig. 5 and thus, the horizontal ULA has the best performance in Fig. 4. Part of the difference between the elevation angles of arrival in the Macro and Micro cell case can be explained with the higher BS in the Macro cell. In a scenario with small elevation angles, the UPA could perform better than the ULA.

The performances with ULA and UPA arrays with the Urban Micro cell channel model are presented in Fig. 6.

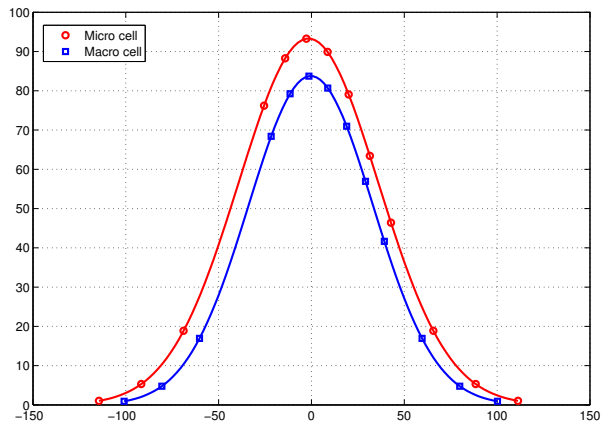


Fig. 5. Distribution of elevation angles of arrival for Urban Macro/Micro cell scenarios.

An 8 degree down tilt angle is used. Results with SINR constraint 0 dB are plotted. The performances of the ULA and UPA with optimal beamforming differ significantly. If the codebook based beamforming is used, the performance degradation compared to the optimal case is significant. If separate weighting vectors for the elevation and azimuth domains are used, the link is not feasible with higher SINR constraints and the maximum transmit power constraint is exceeded. With the SINR constraint of 0 dB, the eigenvector elevation weighting method has the best performance of all the suboptimal methods in the UPA case. It also performs similarly as the codebook based ULA. This is due to the fact that part of the elevation weight vectors are calculated from the channel matrices as in the optimal beamforming case.

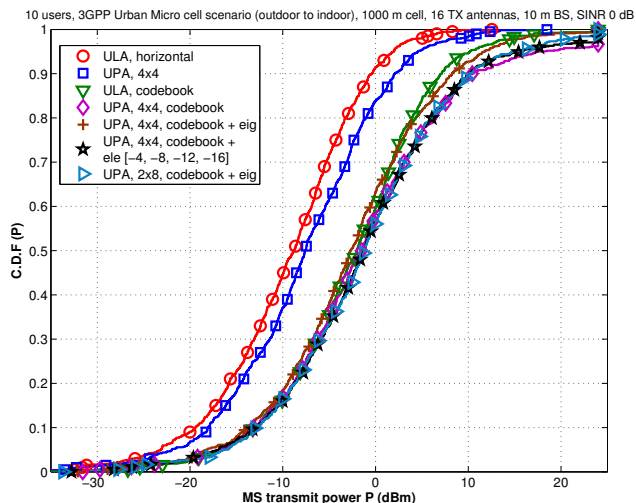


Fig. 6. Transmit power of ULA and UPA with 10 users and Urban Micro cell scenario.

The ULA and UPA performance in the Urban Macro cell scenario are presented in Fig. 7. The down tilt angle is 4

degrees. The differences between the beamforming methods and the antenna arrays are very similar to those in Fig. 6 even though the performance in the Macro cell is better in general. When codebook based beamforming is used, the ULA still outperforms the UPA. Eigenvector based elevation weighting brings performance gain also in the Urban Macro cell scenario.

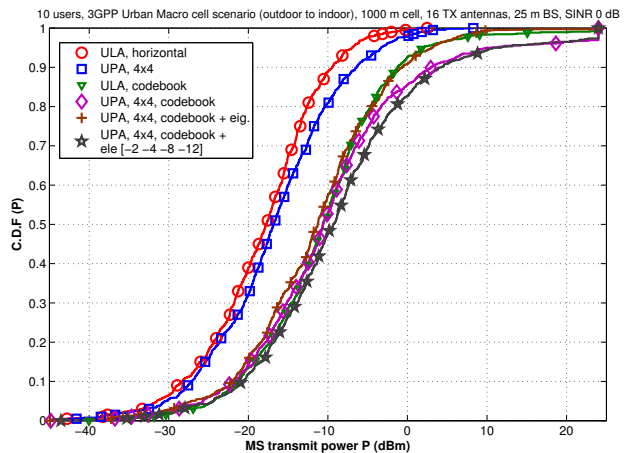


Fig. 7. Transmit power of ULA and UPA with 10 users and Urban Macro cell scenario.

VI. COMPLEXITY ESTIMATIONS

The complexity of the different array processing algorithms presented in Section IV is given here in numbers of operations. The number of operations for each beamforming weight calculation per user in a 16 transmit antenna case is given in Table IV. In the optimal beamforming case, where the beamforming weight vector is given as (12), an $N_i \times N_i$ linear system needs to be solved. In this case, a 16×16 matrix inversion needs to be calculated for every user. In the codebook based method, the weight matrix is suggested by the user and no processing is required at the BS. However, this increases the calculation burden in the user equipment. When the azimuthal codebook is suggested by the user equipment, the BS calculates the best elevation vector, resulting in a low amount of operations. With the eigenvector based elevation weights, an eigenvalue decomposition for a 4×4 matrix is calculated at the BS, assuming 16 transmit antennas. This increases the complexity slightly compared to the fixed elevation weights.

TABLE IV
REQUIRED NUMBER OF OPERATIONS FOR BEAMFORMING WEIGHT CALCULATION

Method	Operations
Optimal beamforming	10260
Codebook based	-
Codebook az., fixed elevation	88
Codebook az., eigenvector elevation	286

VII. CONCLUSIONS

Comparisons between the ULA and UPA were made in terms of their spatial correlation and theoretical beamforming capacity. Network simulations were then performed with the latest 3D channel models to obtain insight into their performance differences. Different array processing algorithms were also utilized.

The ULA was found to outperform the UPA in all the simulated scenarios with optimal beamforming. The results match those given by the theoretical beamforming capacity. A slight increase in performance can be obtained by dividing the processing into azimuth and elevation domains compared to the fixed codebook case. This also gives significant complexity savings in calculating the beamforming weights compared to the optimal beamforming case.

REFERENCES

- [1] J. Koppenborg, H. Halbauer, S. Saur, and C. Hoek, "3D beamforming trials with an active antenna array," in *Proc. Int. ITG Works. on Smart Antennas (WSA)*, Dresden, Germany, Mar. 7–8 2012, pp. 110–114.
- [2] S. K. Yong and J. Thompson, "A three-dimensional spatial fading correlation model for uniform rectangular arrays," *IEEE Antennas Wireless Propagat. Lett.*, vol. 2, no. 1, pp. 182–185, 2003.
- [3] J. Raj, S. Arokiasamy, N. Vikram, and J. Schoebel, "Spatial correlation and MIMO capacity of uniform rectangular dipole arrays," *IEEE Antennas Wireless Propagat. Lett.*, vol. 7, pp. 97–100, May 2008.
- [4] J. Lee and C. Cheng, "The spatial correlation characteristics of 3-D antenna array systems," in *Int. Midwest Symp. on Circuits and Systems (MWSCAS)*, Seoul, South Korea, Aug. 7–10 2011, pp. 1–4.
- [5] M. Narandzic, M. Kaske, C. Schneider, M. Milojevic, M. Landmann, G. Sommerkorn, and R. Thoma, "3D-antenna array model for IST-WINNER channel simulations," in *Proc. IEEE Veh. Technol. Conf.*, Dublin, Ireland, Apr. 22–25 2007, pp. 319–323.
- [6] 3rd Generation Partnership Project (3GPP); Technical Specification Group Radio Access Network, "Study on 3D channel model for LTE (Release 12)," 3rd Generation Partnership Project (3GPP), Tech. Rep., 2014.
- [7] X. Lu, A. Tölli, O. Piirainen, M. Juntti, and W. Li, "Comparison of antenna arrays in a 3-D multiuser multicell network," in *Proc. IEEE Int. Conf. Commun.*, Kyoto, Japan, Jun. 5–9 2011, pp. 1–6.
- [8] P. Kyösti, "Winner II channel models, IST-4-027756 WINNER II, D1.1.2 V1.1," WINNER Project, Tech. Rep., Sep. 2007.
- [9] "Guidelines for evaluation of radio interface technologies for IMT-Advanced," International Telecommunication Union, Tech. Rep.
- [10] B. Friedlander and S. Scherzer, "Beamforming versus transmit diversity in the downlink of a cellular communications system," *IEEE Trans. Veh. Technol.*, vol. 53, no. 4, pp. 1023–1034, Jul. 2004.
- [11] X. Lu, W. Li, A. Tölli, M. Juntti, E. Kunnari, and O. Piirainen, "Joint power control, receiver beamforming and adaptive multi base station coordination for uplink wireless communications," in *Proc. IEEE Int. Symp. Pers., Indoor, Mobile Radio Commun., Workshop on Wireless Distributed Networks*, Sep. 2010, pp. 446 – 450.
- [12] Motorola, "DL codebook design for 8 TX antennas for LTE-A, 3GPP TSG RAN1-56," 3rd Generation Partnership Project (3GPP), Tech. Rep., 2009.
- [13] 3rd Generation Partnership Project (3GPP); Technical Specification Group Radio Access Network, "Evolved universal terrestrial radio access E-UTRA; physical channels and modulation (release 8) TS 36.211 (version 8.5.0)," Tech. Rep., 2008.
- [14] Y. Song, X. Yun, S. Nagata, and L. Chen, "Investigation on elevation beamforming for future LTE-advanced," in *Proc. IEEE Int. Conf. Commun. Workshops*, Budapest, Hungary, Jun.9–13 2013, pp. 106–110.
- [15] T. Thomas and F. Vook, "Transparent user-specific 3D MIMO in FDD using beamspace methods," in *Proc. IEEE Global Telecommun. Conf.*, Anaheim, USA, Dec.3–7 2012, pp. 4618–4623.
- [16] T. Hytönen, "Optimal wrap-around network simulation," Helsinki university of technology, Espoo, Finland, Helsinki university of technology institute of mathematics research reports, 2001.